◆ Human Brain Mapping 38:2398–2407 (2017) ◆

Age-Associated Patterns in Gray Matter Volume, Cerebral Perfusion and BOLD Oscillations in Children and Adolescents

Signe Bray[1,2,3]*

[1]*Departments of Radiology and Pediatrics, Cumming School of Medicine, University of Calgary, 2500 University Ave NW, Calgary AB, T2N1N4, Canada*
[2]*Child and Adolescent Imaging Research (CAIR) Program, 2888 Shaganappi Trail NW, Calgary AB, T3B 6A8, Canada*
[3]*Alberta Children's Hospital Research Institute (ACHRI), 2888 Shaganappi Trail NW, Calgary AB, T3B 6A8, Canada*

Abstract: Healthy brain development involves changes in brain structure and function that are believed to support cognitive maturation. However, understanding how structural changes such as grey matter thinning relate to functional changes is challenging. To gain insight into structure-function relationships in development, the present study took a data driven approach to define age-related patterns of variation in gray matter volume (GMV), cerebral blood flow (CBF) and blood-oxygen level dependent (BOLD) signal variation (fractional amplitude of low-frequency fluctuations; fALFF) in 59 healthy children aged 7–18 years, and examined relationships between modalities. Principal components analysis (PCA) was applied to each modality in parallel, and participant scores for the top components were assessed for age associations. We found that decompositions of CBF, GMV and fALFF all included components for which scores were significantly associated with age. The dominant patterns in GMV and CBF showed significant (GMV) or trend level (CBF) associations with age and a strong spatial overlap, driven by increased signal intensity in default mode network (DMN) regions. GMV, CBF and fALFF additionally showed components accounting for 3–5% of variability with significant age associations. However, these patterns were relatively spatially independent, with small-to-moderate overlap between modalities. Independence of age effects was further demonstrated by correlating individual subject maps between modalities: CBF was significantly less correlated with GMV and fALFF in older children relative to younger. These spatially independent effects of age suggest that the parallel decline observed in global GMV and CBF may not reflect spatially synchronized processes. *Hum Brain Mapp 38:2398–2407, 2017.* © 2017 Wiley Periodicals, Inc.

Key words: magnetic resonance imaging; brain development; multimodal

Additional Supporting Information may be found in the online version of this article.

Contract grant sponsor: NSERC Discovery (S. B.); Contract grant sponsors: Alberta Children's Hospital Foundation and the Sinneave Family Foundation

*Correspondence to: Signe Bray, B4-514 2888 Shaganappi Trail NW, Calgary AB, T3B 6A8, Canada. E-mail: slbray@ucalgary.ca

Received for publication 19 June 2016; Revised 5 November 2016; Accepted 13 December 2016.

DOI: 10.1002/hbm.23526

Published online 24 January 2017 in Wiley Online Library (wileyonlinelibrary.com).

© 2017 Wiley Periodicals, Inc.

INTRODUCTION

The human brain undergoes many changes as it matures from childhood into adulthood [Levitt, 2003]. An overproduction of synapses in early childhood is pruned [Huttenlocher, 1979] and white matter fibers become increasingly myelinated [Yakovlev and Lecours, 1967]. These cellular changes are believed to be reflected in the relatively coarse measurements obtained from in vivo magnetic resonance imaging (MRI). MRI studies have shown an overall decline in gray matter thickness with age [Brown et al., 2012], changes in white matter volume and microstructure [Tamnes et al., 2010] and decline in cerebral blood flow [Chiron et al., 1992; Wintermark et al., 2004], across childhood and adolescence.

These developmental processes unfold at different rates across the brain [Gogtay et al., 2004; Lebel et al., 2008]. Understanding patterns in development is of interest, both to fully characterize typical development and to determine whether brain disorders target "maturational networks" [Alexander-Bloch et al., 2014, 2013; Bray et al., 2015 Krongold et al., 2015]. Associations between structural and functional development have been proposed to occur at the network level: that is, it has been shown that regions which are part of common functional networks mature at similar rates [Raznahan et al., 2011]. However, data-driven approaches to identify structural maturational networks have tended to identify a set of networks in gray and white matter development that do not easily map onto canonical resting-state networks [Alexander-Bloch et al., 2014; Bray et al., 2015; Krongold et al., 2015]. It therefore remains an open question how anatomical changes such as gray matter thinning relate to developmental changes in functional networks and responses. For example, if gray matter thinning is the result of pruning synapses and dendritic spines [Innocenti and Price, 2005], perhaps there is a decline in cortical metabolism that regionally parallels gray matter changes. It has alternatively been suggested that cortical thinning measured with MRI reflects the proliferation of myelin into deep cortical layers [Sowell et al., 2004], in which case regional correspondence between metabolism and thinning may be relatively decoupled.

Towards addressing this question, the present study used a data-driven approach to examine how patterns of gray matter volume (GMV) vary with age, and asked if there was overlap with age-related patterns in cerebral hemodynamics. We used T1-weighted MR images to quantify regional GMV while functional measures included both arterial spin labeling (ASL) to derive maps of cerebral blood flow (CBF) and the fractional amplitude of low frequency fluctuations (fALFF) derived from blood oxygen level dependent (BOLD) functional MRI (fMRI). fALFF is a measure of fMRI BOLD signal variability that is believed to be sensitive to both vascular reactivity [Di et al., 2012] and spontaneous neuronal activity [Zou et al., 2008].

We hypothesized that changes in GMV would show a developmental pattern that divides anterior from posterior brain regions, consistent with our previous work [Bray et al., 2015; Krongold et al., 2015]. We further hypothesized that similar patterns would be apparent in CBF and fALFF measures, as CBF has similarly been shown to globally decline with age following a peak in early childhood [Avants et al., 2015; Biagi et al., 2007; Chiron et al., 1992; Wang and Licht, 2006; Wintermark et al., 2004], that parallels what is seen in global GMV.

MATERIALS AND METHODS

Participants

Data from the pediatric template of brain perfusion [Avants et al., 2015] were analyzed for this study. This data set includes neuroimaging and demographic data for 120 participants aged 7–20 years. For several participants, more than one time point was acquired. We chose a subset of participants/timepoints for whom (criteria applied in order): (1) demographic data were available ($N = 120$), (2) T1, ASL and fMRI data were available ($N = 108$ remaining), (3) if repeated measures were available, we chose the functional run with the lesser amount of head motion, and motion being equal chose the younger available age, only participants with at least 150 volumes of usable fMRI data were included ($N = 71$), (4) functional images had good coverage ($N = 67$), (5) no artifact in ASL images by visual inspection ($N = 64$), (6) T1 quality was rated as usable by visual inspection ($N = 59$). After applying these criteria, our final analysis included 59 participants (34 female) aged 7–18 years (mean = 13.8, st.dev.=3.12), mean IQ = 109.3 (range = 81–147, st.dev.=24).

As described in Avants et al. [2015], typically developing children were recruited into this study at the Ahmanson-Lovelace Brain Mapping Center at UCLA, by the Laboratory of Functional MRI Technology (LOFT). Exclusion criteria included: (1) previous diagnosis of medical condition, developmental, psychiatric or learning disorder; (2) currently meeting criteria for a learning/psychiatric or neurological condition; (3) exposed to environmental conditions likely to impact normal development; (4) MRI contraindications; (5) limited English proficiency. Full exclusion criteria are listed in Supporting Information Table I. Written informed consent to participate in the study and public release of the data was obtained from each subject and their parents according to the Institutional Review Board (IRB) of University of California Los Angeles (UCLA) guidelines prior to IQ assessment and MR scans.

T1-Weighted Image Acquisition and Processing

Magnetization-Prepared Rapid Acquisition Gradient Echo (MPRAGE) images were acquired using a 3D inversion recovery sequence with TR/TE/TI = 2,170/4.33/1,100 ms, $1 \times 1 \times 1$ mm^3 resolution with a matrix size of 256 $\times$

256 × 192. The flip angle = 7° for a total scan time of 8:08 min. T1 images were entered into a voxel based morphometry (VBM) pipeline in the SPM12 MATLAB (Mathworks, Natick, MI) software. Steps included segmentation and normalization using a custom template generated with the DARTEL Toolbox [Ashburner, 2007]. Normalized gray and white matter segmented images were modulated to "preserve amounts" and smoothed using an 8mm Gaussian kernel. All segmentations were visually inspected prior to analysis.

ASL-CBF Image Acquisition and Processing

Pseudo continuous arterial spin labeled (pCASL) images were acquired using gradient-echo echo-planar imaging (EPI) with TR/TE = 4,000/12 ms. The resolution is 3.125 × 3.125 × 6 mm (5 mm with 1 mm gap) over a 64 × 64 × 24 matrix. 40 label/control pairs were acquired. Generalized autocalibrating partially parallel acquisition (GRAPPA) was used with an acceleration factor of 2. Labeling duration was 1.5 s and the postlabeling delay was 1.2 s. Total imaging time was 5:30 min. CBF maps were calculated from ASL images, as described in [Avants et al., 2015]. Specifically, each subject's M0 image, obtained as the mean of the control images, was warped to the subject's T1 image using the antsIntermodalityIntrasubject.sh script. These transforms were concatenated with the subject-to-template transforms to warp the template labels to the subject native ASL space. The M0 image served as a reference for motion-correction of all time-point volumes. In addition to the motion and nuisance regressors described above, either the tag or control label of the image was included as a regressor, with the coefficient of that regressor corresponding to the average difference between tag and control. All regressors were included in a robust regression scheme for CBF calculation [Avants et al., 2012]. The equation for CBF calculation can be found in [Wu et al., 2010] with an assumed labeling efficiency of 0.85. Full details are available in the open-source script at https://raw.github.com/stnava/ANTs/master/Scripts/antsASLProcessing.sh. The blood T1 value was adjusted for age and gender as T1=(2115.6–21.5*age-73.3*sex) ms, where female sex was set to 0 and male was set to 1, as suggested in [Wu et al., 2010]. CBF map preprocessing was performed in SPM12 and included registration to the participant's T1-weighted image, normalization to the MNI template using DARTEL-derived flow fields and spatial smoothing with a 8mm FWHM kernel.

BOLD fMRI Acquisition and fALFF Processing

Blood oxygen level-dependent (BOLD) images were acquired in the resting state using 2D EPI with TR/TE = 2,000/27 ms. The resolution is 4 × 4 × 4 mm over a 64 × 64 × 25 matrix and up to 244 time points were acquired. The flip angle = 80°. Subjects were required to relax quietly while looking at a fixation point. No physiological monitoring was performed or explicit verification of wakefulness. Data were preprocessed in SPM12 using a standard pipeline that included slice-time correction and realignment to the first functional volume in the series. Images were normalized to MNI space using DARTEL-derived flow fields and smoothed with an 8mm FWHM kernel. Art software (https://www.nitrc.org/projects/artifact_detect/) was used to flag volumes with greater than 0.2 mm framewise displacement. From pre-processed images, an fALFF map was calculated for each person using the DPARSF toolbox [Chao-Gan and Yu-Feng, 2010]. fALFF calculates the power at low-frequency (0.01–0.08 Hz) at each voxel, relative to all frequencies and is less sensitive to artefacts than the non-normalized ALFF measure [Zou et al., 2008]. Volumes flagged by the Art toolbox were excluded during this calculation.

PCA and Age-Associated Components

A group gray matter mask was derived by averaging the segmented images, thresholding at 0.75 and masking by regions covered in BOLD ALFF images. This mask was used to extract values from the processed GMV maps, the CFB maps and the fALFF maps for each subject. These were used to create a set of three matrices (subject × voxel) which were entered into a PCA for each modality.

Across all three modalities, the first principal component accounted for over 40% of the variance. As this study had limited power, we examined only the components accounting for 2.5% or more of the total variance (2 GMV, 4 CBF and 3 fALFF components); this level was chosen by plotting the variance explained by each component and locating elbows in the plots (Supporting Information Fig. 1). In these components we assessed whether component scores were significantly associated with age, controlling for sex and propensity for head motion (estimated from the functional run [Alexander-Bloch et al., 2016])—all three parameters were included simultaneously in the models. Follow-up models assessed whether age^2 and age × sex interaction terms explained significant variance in the scores.

Associations between Components

In order to compare the topography of derived components, spatial correlations were calculated across gray matter voxels between each age-associated pair of components. Note that due to the large number of voxels (N = 143488), all spatial correlations are highly significant, but vary in effect size. Correlations were also calculated between component scores, with and without controlling for shared effects of age. In addition to examining similarity in expression of principal components, correlations were calculated between maps of different modalities

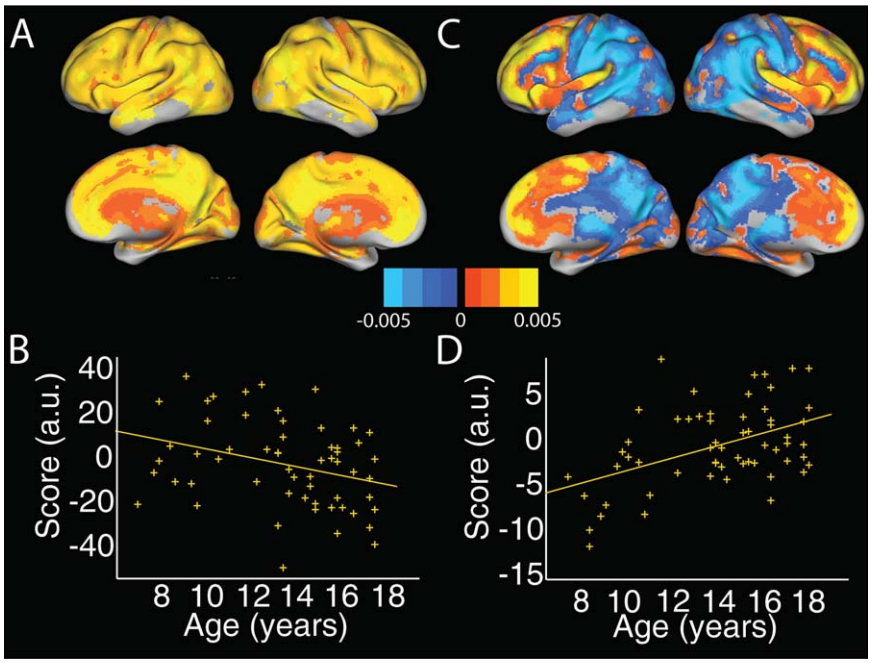

Figure 1.

Two age-associated principal components in GMV. (**a**) Spatial distribution and (**b**) associated scores plotted against age for the top principal component, accounting for 51.9% of the variance. This component showed regions of higher intensity in DMN regions such as posterior and anterior cingulate. (**c**) Spatial distribution and (**d**) associated scores plotted against age for the second principal component, accounting for 2.9% of the variance. This component showed a separation between anterior and posterior cortical regions. GMV = gray matter volume; DMN = default mode network. [Color figure can be viewed at wileyonlinelibrary.com]

within individuals; intermodality correlation values were tested for associations with age.

RESULTS

Age-Associated GMV Components

Global GMV was entered into a multiple linear regression with age, sex and motion estimated from the functional run. As expected, global GMV showed a significant decline with age ($t(55) = -2.67$, $P < 0.05$), and a significant association with sex ($t(55)=4.6$, $P < 0.001$), but not with head motion ($P > 0.5$). Neither age^2 nor age × sex interaction terms were significant when added, separately, to this model, perhaps due to insufficient sample size.

In the PCA analysis, the top two principal components accounted for 51.9% and 2.9% of the variance respectively; subsequent components accounted for less than 2.5% and were not considered further. *P*-values reported are Holm–Bonferroni adjusted for 2 comparisons. The first component showed significant associations with age ($t(55) = -2.77$, $P < 0.05$; Fig. 1a,b). This component encompassed most of the cortex; some regions of higher intensity coincided with the default mode network, that is, precuneus, inferior parietal lobule and anterior cingulate, in addition to dorsal prefrontal and anterior temporal regions. The second component also showed significant associations with age ($t(55) = 3.6$, $P < 0.005$; Fig. 1c,d), and broadly distinguished regions anterior to the precentral gyrus from posterior, with scores suggesting a steeper decline in posterior cortex. We note that both age-associated components also showed a significant association with sex ($t(55) = 4.6$, $P < 0.005$ and $t(55) = 2.6$, $P < 0.05$). Age^2 and age × sex interaction terms were not significant when added to the models.

Age-Associated ASL-CBF Components

Similar to GMV, global CBF showed a significant decline with age ($t(55) = -2.16$, $P < 0.05$). However, sex and head motion were not significant predictors (both $P > 0.3$). Neither age^2 nor age × sex interaction terms were significant when added, separately, to this model.

The top four principal components accounted for 40.6%, 5.9%, 3.7% and 3% of the variance, respectively. *P*-values reported are Holm–Bonferroni adjusted for four comparisons. The first principal component showed a trend level association with age ($t(55) = -2.3$, $P = 0.06$; Fig. 2a,b), while the fourth principal component showed a significant association with age ($t(55) = -3.3$, $P < 0.01$; Fig. 2c,d). Similar to

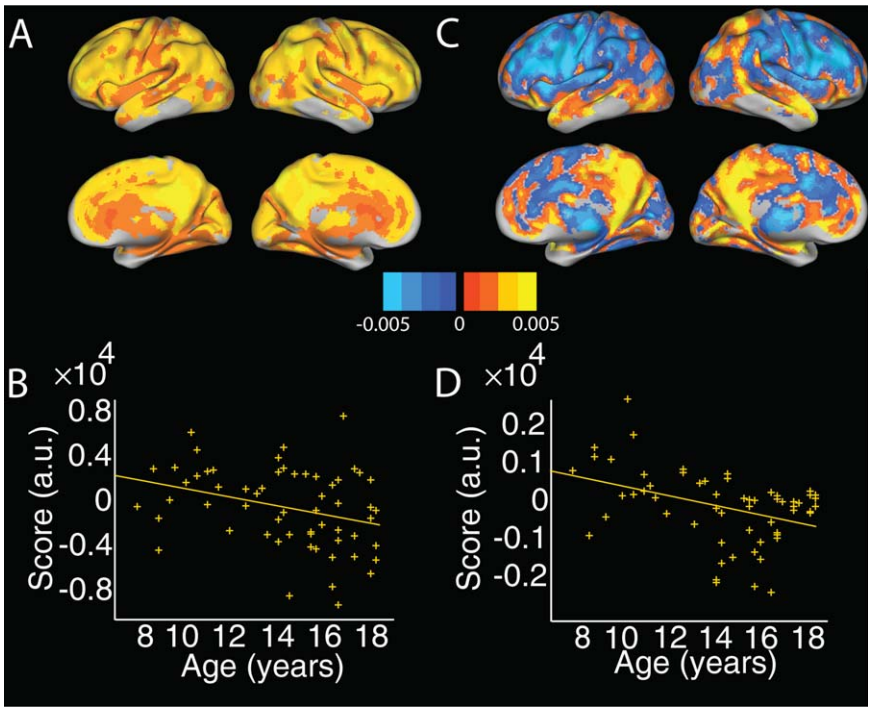

Figure 2.

Two age-associated principal components in CBF. (**a**) Spatial distribution and (**b**) associated scores plotted against age for the top principal component, accounting for 40.6% of the variance. This component includes regions of high intensity in the posterior cingulate/precuneus. Note component scores showed only a trend-level association with age ($P = 0.06$). (**c**) Spatial distribution and (**d**) associated scores plotted against age for the fourth principal component, accounting for 3% of the variance. This component distinguished medial and lateral parietal cortex from dorsal/lateral prefrontal regions. CBF = cerebral blood flow. [Color figure can be viewed at wileyonlinelibrary.com]

GMV, the first CBF component covered most of the cortex, with higher intensity in several default mode regions. The fourth principal component distinguished medial and lateral parietal cortex, with temporal cortex, from cingulate and lateral frontal regions. Only the third principal component showed a significant association with sex ($t(55) = -3.8$, $P < 0.01$). Neither age^2 nor age × sex interaction terms were significant when added to the models.

Age-Associated BOLD-fALFF Components

Global fALFF did not show a significant effect of age, sex, head motion age^2 or age × sex interaction (all $P < 0.25$). The top 3 fALFF components accounted for 41.5%, 5.2% and 4.16% of the variance, respectively. Only the second fALFF component showed a significant association with age ($t(55) = -2.6$, $P < 0.05$; Fig. 3a,b). This component distinguished posterior regions that included occipital, parietal and sensorimotor regions (in cool colors), from anterior regions including inferior parietal, insular, anterior and posterior cingulate (in warm colors). Several of the warm-colored regions overlap with default mode (precuneus, inferior parietal lobule, medial prefrontal cortex) and salience network regions (insular cortex, cingulate gyrus), with scores indicating a greater age-related decline in these regions. No components showed a significant association with sex. Neither age^2 nor age × sex interaction terms were significant when added to the models.

GMV and CBF

While the top GMV and CBF components had a strong spatial overlap ($r = 0.59$, $P < 10^{-10}$), overlap was modest for the remaining component pairs (small effect sizes; $|r| = 0.12$–0.19).

Across subjects, scores for the top components were not significantly correlated ($P = 0.3$) nor were the two age-associated components (GMV #2 and CBF #4), though they did show a trend ($r = -0.22$, $P = 0.09$). This trend-level effect was mediated by a shared effect of age ($r = -0.05$, $P = 0.69$, partial correlation controlling for age). When stratifying by sex, in the male subjects only the top components were significantly correlated ($r = 0.5$, $P < 0.05$); this effect was not significant in the female subjects ($P = 1$).

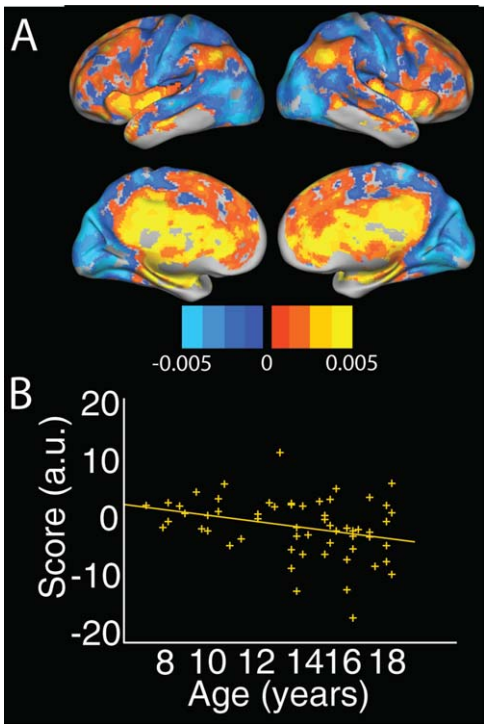

Figure 3.
One age-associated principal component in fALFF. (**a**) Spatial distribution and (**b**) associated scores plotted against age for the second fALFF component, accounting for 5.2% of the variance. This component distinguished DMN and salience network regions from occipital, superior parietal and pre/post central gyrus regions. fALFF = fractional amplitude of low frequency fluctuations; DMN = default mode network. [Color figure can be viewed at wileyonlinelibrary.com]

We further examined the spatial similarity in GMV and CBF maps across subjects. We found a high correlation on average ($r = 0.6725$, range 0.44–0.71). The distribution of permuted values ranged from 0.33 to 71 with a mean of 0.75; 37% of subjects showed correlation values exceeding the 95th percentile. We found a trend level association between age and GMV-CBF correlation ($r = -0.24$, $P = 0.07$); after removing one outlier with a correlation value more than 2.5 standard deviations below the mean, the association with age was significant ($r = -0.27$, $P = 0.04$; Fig. 4a). Together this suggests that while GMV and CBF are highly correlated at the population level, likely due to prominent anatomical features, effects of age are relatively spatially independent between these two modalities, leading to reduced intermodality correlations with increasing age.

GMV and fALFF

GMV and fALFF components showed modest spatial overlap ($|r| = 0.13$–0.23). The strongest overlap was seen between the second GMV component and the fALFF component, likely reflecting a tendency for both components to distinguish anterior from posterior brain regions.

Correlation with fALFF scores was significant for both GMV components (Holm–Bonferroni corrected $P < 0.05$). These are no longer significant after controlling for age ($P > 0.1$), suggesting that age mediates this effect. Stratifying by sex, in the male subjects the correlation with GMV #1 only remains significant ($r = 0.55$, $P < 0.01$); neither correlation is significant in the female subjects ($P = 0.3$,0.1).

On average, the correlation between participants' fALFF and GMV maps was 0.3 (range: 0.13–0.44). The correlation between group averaged maps was $r = 0.42$. The distribution of permuted values ranged from 0.1 to 0.44 with a mean of 0.27; 12% of subjects showed correlation values

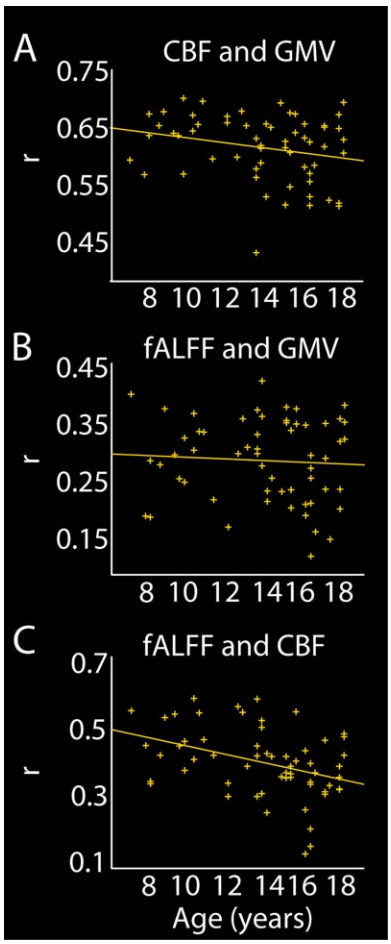

Figure 4.
Intermodal correlations and their association with age. (**a**) Intermodal correlations between CBF and GMV maps calculated for each subject and plotted against age, with regression line. (**b**) Intermodal correlations between fALFF and GMV maps calculated for each subject and plotted against age, with regression line. (**c**) Intermodal correlations between fALFF and CBF maps calculated for each subject and plotted against age, with regression line. [Color figure can be viewed at wileyonlinelibrary.com]

exceeding the 95th percentile. There was no association between intermodal correlations and age (Fig. 4b). Together these results suggest that while the spatial overlap between fALFF and GMV components is modest, there are some shared effects of age on interindividual variability in these two modalities.

fALFF and CBF

CBF and fALFF components showed low spatial overlap ($|r| = 0.012–0.15$). Scores were significantly correlated for the first CBF component and the fALFF component ($r = 0.31$, $P < 0.05$); this relationship was no longer significant in a partial correlation controlling for age. Stratifying by sex, this correlation is significant only in the male subjects ($r = 0.4$, $P < 0.05$). The correlation between individual subjects' fALFF and CBF maps was on average $r = 0.42$ (range: 0.15–0.61); correlation between group averaged maps was 0.65. The distribution of permuted values ranged from 0.13 to .55 with a mean of 0.35; 22% of subjects showed correlation values exceeding the 95th percentile. The intermodality correlation showed a significant decline with increasing age ($r = -0.38$, $P < 0.005$; Fig. 4c). Thus, similar to the GMV-CBF comparison, a diverging pattern of age effects may lead to reduced correlation between fALFF and CBF with increasing age.

DISCUSSION

The goal of this study was to assess and compare age-associated patterns in GMV and cerebral hemodynamics. We found that decompositions of CBF, GMV and fALFF all included components for which scores were significantly associated with age. The dominant patterns in GMV and CBF showed significant (GMV) or trend level (CBF) associations with age and a strong spatial overlap, largely driven by increased signal intensity in DMN regions. GMV, CBF and fALFF additionally showed components accounting for 3–5% of variability with significant age associations. However, these patterns were relatively spatially independent, with small-to-moderate overlap between modalities. Relative spatial independence of age effects was further demonstrated by correlating individual subject maps between modalities: CBF was less correlated with GMV and fALFF in older children relative to younger. These independent effects of age support previous studies using multivariate predictions to determine participants' age [Avants et al., 2015; Brown et al., 2012], as these also show increased accuracy with multi-modal inputs. Further, this work suggests that longitudinal measurements and more complex models will be necessary to fully understand how developmental changes in brain structure relate to changes in function.

The top principal component in both GMV and CBF showed high intensity in the precuneus/posterior cingulate, a core node in the DMN [Fox et al., 2005], with a strong spatial overlap between components ($r = 0.59$). These components showed a significant association with age for GMV and trend-level for CBF, but individual scores were not significantly correlated. CBF and fALFF have previously been shown to have higher amplitude in DMN regions [Zou et al., 2009]. The DMN contains some of the brain's most connected regions, both functionally [Cole et al., 2010] and structurally [Hagmann et al., 2008], and has a high baseline metabolic rate [Raichle et al., 2001]. Regions of the DMN have been shown to increase in coupling with childhood maturation [Sato et al., 2014; Sherman et al., 2014] and become increasingly segregated from other networks [Chai et al., 2014]. This increase in connectivity and specialization is a reduction in gray mater volume is consistent with the suggestion that synaptic and dendritic pruning [Huttenlocher, 1979] both contribute to gray matter thinning and reflect a refining of neural networks with development.

The finding that cortical GMV declines with age across late childhood and adolescence has been extensively replicated [Giedd et al., 1999; Gogtay et al., 2004; Sowell et al., 2004]. However, only recently have studies begun to consider inter-regional coordination in developmental patterns [Raznahan et al., 2011; Zielinski et al., 2010]. This work is exciting in that it may identify networks of regions that are targeted by specific brain disorders [Alexander-Bloch et al., 2014; Douaud et al., 2014;]. We found here that the most prominent age-associated GMV component distinguished anterior prefrontal (PFC) from posterior cortical regions, with associated scores suggesting a more pronounced decline in posterior volume across this age range. This is consistent with two recent studies from our group, using different methods applied to a separate dataset [Bray et al., 2015; Krongold et al., 2015], and with early descriptions of cortical developmental patterns which showed a more protracted trajectory for prefrontal regions [Gogtay et al., 2004]. This anterior/posterior distinction in volume may be largely driven by ongoing expansion of surface area in the prefrontal cortex up to early adolescence [Krongold et al., 2015]. Interestingly, this anterior/posterior separation is mirrored in studies using automated clustering to group regions with similar genetic influence on surface area [Chen et al., 2012].

While convergent literature shows a decline in global CBF with age across childhood [Avants et al., 2015; Biagi et al., 2007; Chiron et al., 1992; Wang and Licht, 2006; Wintermark et al., 2004], a smaller number of studies have mapped voxel- or vertex-wise trajectories. The fourth CBF component, which was significantly associated with age, distinguished medial and lateral parietal lobe from the remainder of the brain. Scores suggest a steeper age-related decline in CBF in these parietal association regions. Consistent with this finding, it has previously been shown that association regions, including the posterior parietal cortex, show a steep CBF decline in childhood relative to primary sensory regions [Satterthwaite et al., 2014].

While we hypothesized that age-associated patterns would be similar between GMV and CBF based on both measures sharing a global decline across the age range studied, spatial overlap for age-associated patterns was modest and scores were correlated only at a trend-level. However, it is notable that both components suggest a pronounced decline in both medial and lateral parietal lobe. In CBF these regions are relatively isolated while in GMV the component includes occipito-temporal and post-central gyral regions. Nonetheless, this parietal overlap highlights the pronounced developmental changes in this region across late childhood and suggests that this site may be useful for future studies of the mechanisms underlying structure–function relationships in development. The age-associated fALFF component showed a similar tendency to GMV to distinguish posterior from anterior cortical regions. However a striking difference, likely contributing to the modest spatial overlap ($r = 0.23$), is that in fALFF regions of the DMN were not included in the posterior component. Also notable is the opposing direction of effects: in fALFF DMN + anterior regions showed a more pronounced decline, relative to non-DMN posterior regions. The fALFF component showed limited spatial similarity to CBF components.

The one fALFF component showing a significant association with age distinguished DMN (precuneus, inferior parietal cortex and anterior cingulate/medial prefrontal cortex) and salience network (insular cortex, medial cingulate) from occipital, temporal, superior parietal and pre/post central gyral regions. This component accounted for a smaller proportion of the variance (5.2%) than GMV components (55%), or CBF components (42%) suggesting that fALFF measures may be less sensitive to age. It has previously been shown that while both resting and task-based CBF amplitudes are larger in younger children relative to older children and adults, the normalized BOLD response is not significantly different between these age groups [Moses et al., 2014]. Thus, measures derived from BOLD fluctuations may show a lower sensitivity to age. It is interesting to note that despite some discussion of the precise timing of the onset of gray matter decline [Walhovd et al., 2016], the literature on gray matter changes in the brain has been relatively consistent. Similarly, a global decline in CBF is widely replicated [Avants et al., 2015; Biagi et al., 2007; Chiron et al., 1992; Wang and Licht, 2006; Wintermark et al., 2004]. In contrast, the trajectory of functional development is less straightforward and functional connectivity studies in particular have been challenged by the pernicious effects of head motion [Power et al., 2012].

To complement PCA-based analyses, we also directly correlated both individual subject and group averaged maps between modalities, and examined changes in intermodal correlations with age. At the group averaged level, the strongest intermodal similarity was between GMV and CBF, followed by fALFF and CBF and finally fALFF and GMV. Interestingly, when correlating individual subject maps between modalities, both CBF-GMV and CBF-fALFF showed correlations that were weaker in older children, suggesting a decoupling of cerebral metabolism from gray matter structure with increasing age. It has been suggested that changes in perfusion that cannot be explained by changes in neuroanatomy represent development of functional specialization [Kandel et al., 2015]. In a recent study [Kandel et al., 2015], perfusion that was unexplained by anatomy (i.e., residual) showed a significant effect of age in hippocampal and default mode network regions, but not occipital or precentral gyrus regions which have been suggested to develop earlier [Gogtay et al., 2004].

While strengths of this study include the use of a unique multi-modal neuroimaging resource, this study has several limitations. This study was cross-sectional, while longitudinal data would enable a more direct comparison of change in each modality. The fALFF reflects the relative contribution of low-frequency power to the overall signal in a given voxel, but the meaning of this signal in terms of vascular relative to "neural" contributions is unclear. This measure may also be less reliable than CBF or GMV [Mao et al., 2015; Zuo et al., 2010]. The analytic method used here revealed spatial components that accounted for variability in the data, several of which were associated with participants' age. However, other methods such as parallel ICA [Liu et al., 2009] may be better suited to identifying linked components in different modalities. Finally, spatial smoothing inflates the value of correlations across modalities; however, when repeating the age-correlation analysis on unsmoothed images the significant decline with age in CBF-GMV and CBF-fALFF correlations remained significant.

In summary, this study investigated age-associated patterns in GMV, CBF and fALFF and relationships between them. We found components in each modality that were significantly associated with age, but that the spatial topography of these patterns was largely independent between modalities. A notable exception is a parallel decline in parietal GMV and CBF in medial and lateral parietal regions. Correlations between subject maps of different modalities further showed that CBF maps become less similar to GMV and fALFF maps in older children, further suggesting relatively independent effects of age. Our findings suggest that the parallel decline observed in global GMV and CBF values should not necessarily be interpreted as reflecting spatially synchronized processes and that further work is required to understand the relationships between functional and structural brain development.

ACKNOWLEDGMENTS

We would like to acknowledge the families who participated in the PTBP study for generously agreeing that their data be included in this shared resource, and the study

authors for creating this valuable data set. The author has no conflicts of interest to declare.

REFERENCES

Alexander-Bloch A, Raznahan A, Bullmore E, Giedd J (2013): The convergence of maturational change and structural covariance in human cortical networks. J Neurosci 33:2889–2899.

Alexander-Bloch AF, Reiss PT, Rapoport J, McAdams H, Giedd JN, Bullmore ET, Gogtay N (2014): Abnormal cortical growth in schizophrenia targets normative modules of synchronized development. Biol Psychiatry 76:438–446.

Alexander-Bloch A, Clasen L, Stockman M, Ronan L, Lalonde F, Giedd J, Raznahan A (2016): Subtle in-scanner motion biases automated measurement of brain anatomy from in vivo MRI. Hum Brain Mapp 37:2385–2397.

Ashburner J (2007): A fast diffeomorphic image registration algorithm. Neuroimage 38:95–113.

Avants BB, Lakshmikanth SK, Duda JT, Detre JA, Grossman M (2012): Robust cerebral blood flow reconstruction from perfusion imaging with an open-source, multi-platform toolkit. In Proceedings of Perfusion MRI: Standardization, Beyond CBF and Everyday Clinical Applications, International Society for Magnetic Resonance in Medicine Scientific Workshop (Amsterdam).

Avants BB, Duda JT, Kilroy E, Krasileva K, Jann K, Kandel BT, Tustison NJ, Yan L, Jog M, Smith R, Wang Y, Dapretto M, Wang DJ (2015): The pediatric template of brain perfusion. Sci Data 2:150003.

Biagi L, Abbruzzese A, Bianchi MC, Alsop DC, Del Guerra A, Tosetti M (2007): Age dependence of cerebral perfusion assessed by magnetic resonance continuous arterial spin labeling. J Magn Reson Imaging 25:696–702.

Bray S, Krongold M, Cooper C, Lebel C (2015): Synergistic effects of age on patterns of white and gray matter volume across childhood and adolescence (1,2,3). eNeuro 2.

Brown TT, Kuperman JM, Chung Y, Erhart M, McCabe C, Hagler DJ, Venkatraman VK, Akshoomoff N, Amaral DG, Bloss CS, Casey BJ, Chang L, Ernst TM, Frazier A, Gruen JR, Kaufmann WE, Kenet T, Kennedy DN, Murray SS, Sowell ER, Jernigan TL, Dale AM (2012): Neuroanatomical assessment of biological maturity. Curr Biol 22:1693–1698.

Chai XJ, Ofen N, Gabrieli JD, Whitfield-Gabrieli S (2014): Selective development of anticorrelated networks in the intrinsic functional organization of the human brain. J Cogn Neurosci 26: 501–513.

Chao-Gan Y, Yu-Feng Z (2010): DPARSF: A MATLAB toolbox for "pipeline" data analysis of resting-state fMRI. Front Syst Neurosci 4:13.

Chen CH, Gutierrez ED, Thompson W, Panizzon MS, Jernigan TL, Eyler LT, Fennema-Notestine C, Jak AJ, Neale MC, Franz CE, Lyons MJ, Grant MD, Fischl B, Seidman LJ, Tsuang MT, Kremen WS, Dale AM (2012): Hierarchical genetic organization of human cortical surface area. Science 335:1634–1636.

Chiron C, Raynaud C, Mazière B, Zilbovicius M, Laflamme L, Masure MC, Dulac O, Bourguignon M, Syrota A (1992): Changes in regional cerebral blood flow during brain maturation in children and adolescents. J Nucl Med 33:696–703.

Cole MW, Pathak S, Schneider W (2010): Identifying the brain's most globally connected regions. Neuroimage 49: 3132–3148.

Di X, Kannurpatti SS, Rypma B, Biswal BB (2012): Calibrating BOLD fMRI activations with neurovascular and anatomical constraints. Cereb Cortex. 23:255–263.

Douaud G, Groves AR, Tamnes CK, Westlye LT, Duff EP, Engvig A, Walhovd KB, James A, Gass A, Monsch AU, Matthews PM, Fjell AM, Smith SM, Johansen-Berg H (2014): A common brain network links development, aging, and vulnerability to disease. Proc Natl Acad Sci USA 111:17648–17653.

Fox MD, Snyder AZ, Vincent JL, Corbetta M, Van Essen DC, Raichle ME (2005): The human brain is intrinsically organized into dynamic, anticorrelated functional networks. Proc Natl Acad Sci USA 102:9673–9678.

Giedd JN, Blumenthal J, Jeffries NO, Castellanos FX, Liu H, Zijdenbos A, Paus T, Evans AC, Rapoport JL (1999): Brain development during childhood and adolescence: A longitudinal MRI study. Nat Neurosci 2:861–863.

Gogtay N, Giedd JN, Lusk L, Hayashi KM, Greenstein D, Vaituzis AC, Nugent TF, Herman DH, Clasen LS, Toga AW, Rapoport JL, Thompson PM (2004): Dynamic mapping of human cortical development during childhood through early adulthood. Proc Natl Acad Sci USA 101:8174–8179.

Hagmann P, Cammoun L, Gigandet X, Meuli R, Honey CJ, Wedeen VJ, Sporns O (2008): Mapping the structural core of human cerebral cortex. PLoS Biol 6:e159.

Huttenlocher PR (1979): Synaptic density in human frontal cortex - developmental changes and effects of aging. Brain Res 163: 195–205.

Innocenti GM, Price DJ (2005): Exuberance in the development of cortical networks. Nat Rev Neurosci 6:955–965.

Kandel BM, Wang DJ, Detre JA, Gee JC, Avants BB (2015): Decomposing cerebral blood flow MRI into functional and structural components: A non-local approach based on prediction. Neuroimage 105:156–170.

Krongold M, Cooper C, Bray S (2015): Modular development of cortical gray matter across childhood and adolescence. Cereb Cortex ePub ahead of print.

Lebel C, Walker L, Leemans A, Phillips L, Beaulieu C (2008): Microstructural maturation of the human brain from childhood to adulthood. Neuroimage 40:1044–1055.

Levitt P (2003): Structural and functional maturation of the developing primate brain. J. Pediatr 143:S35–S45.

Liu J, Pearlson G, Windemuth A, Ruano G, Perrone-Bizzozero NI, Calhoun V (2009): Combining fMRI and SNP data to investigate connections between brain function and genetics using parallel ICA. Hum Brain Mapp 30:241–255.

Mao D, Ding Z, Jia W, Liao W, Li X, Huang H, Yuan J, Zang YF, Zhang H (2015): Low-frequency fluctuations of the resting brain: High magnitude does not equal high reliability. PLoS One 10:e0128117.

Moses P, Dinino M, Hernandez L, Liu TT (2014): Developmental changes in resting and functional cerebral blood flow and their relationship to the BOLD response. Hum Brain Mapp 35: 3188–3198.

Power JD, Barnes KA, Snyder AZ, Schlaggar BL, Petersen SE (2012): Spurious but systematic correlations in functional connectivity MRI networks arise from subject motion. Neuroimage 59:2142–2154.

Raichle ME, MacLeod AM, Snyder AZ, Powers WJ, Gusnard DA, Shulman GL (2001): A default mode of brain function. Proc Natl Acad Sci USA 98:676–682.

Raznahan A, Lerch JP, Lee N, Greenstein D, Wallace GL, Stockman M, Clasen L, Shaw PW, Giedd JN (2011): Patterns of coordinated anatomical change in human cortical

development: A longitudinal neuroimaging study of maturational coupling. Neuron 72:873–884.

Sato JR, Salum GA, Gadelha A, Picon FA, Pan PM, Vieira G, Zugman A, Hoexter MQ, Anés M, Moura LM, Gomes Del'Aquilla MA, Amaro E, McGuire P, Crossley N, Lacerda A, Rohde LA (2014): Age effects on the default mode and control networks in typically developing children. J Psychiatr Res 58: 89–95.

Satterthwaite TD, Shinohara RT, Wolf DH, Hopson RD, Elliott MA, Vandekar SN, Ruparel K, Calkins ME, Roalf DR, Gennatas ED, Jackson C, Erus G, Prabhakaran K, Davatzikos C, Detre JA, Hakonarson H, Gur RC, Gur RE (2014): Impact of puberty on the evolution of cerebral perfusion during adolescence. Proc Natl Acad Sci USA 111:8643–8648.

Sherman LE, Rudie JD, Pfeifer JH, Masten CL, McNealy K, Dapretto M (2014): Development of the default mode and central executive networks across early adolescence: A longitudinal study. Dev Cogn Neurosci 10:148–159.

Sowell ER, Thompson PM, Leonard CM, Welcome SE, Kan E, Toga AW (2004): Longitudinal mapping of cortical thickness and brain growth in normal children. J Neurosci 24:8223–8231.

Tamnes CK, Ostby Y, Fjell AM, Westlye LT, Due-Tønnessen P, Walhovd KB (2010): Brain maturation in adolescence and young adulthood: Regional age-related changes in cortical thickness and white matter volume and microstructure. Cereb Cortex 20:534–548.

Walhovd KB, Fjell AM, Giedd J, Dale AM (2016): Through thick and thin: A need to reconcile contradictory results on trajectories in human cortical development. Cereb Cortex ePub ahead of print.

Wang J, Licht DJ (2006): Pediatric perfusion MR imaging using arterial spin labeling. Neuroimaging Clin N Am 16:149–167, ix.

Wintermark M, Lepori D, Cotting J, Roulet E, van Melle G, Meuli R, Maeder P, Regli L, Verdun FR, Deonna T, Schnyder P, Gudinchet F (2004): Brain perfusion in children: Evolution with age assessed by quantitative perfusion computed tomography. Pediatrics 113:1642–1652.

Wu WC, Jain V, Li C, Giannetta M, Hurt H, Wehrli FW, Wang DJ (2010): In vivo venous blood T1 measurement using inversion recovery true-FISP in children and adults. Magn Reson Med 64:1140–1147.

Yakovlev PI, Lecours AR (1967): The myelogenetic cycles of regional maturation of the brain. In Regional Development of the Brain in Early Life, Minkowski ed. Oxford: Blackwell. pp 3–70.

Zielinski BA, Gennatas ED, Zhou J, Seeley WW (2010): Network-level structural covariance in the developing brain. Proc Natl Acad Sci USA 107:18191–18196.

Zou Q, Wu CW, Stein EA, Zang Y, Yang Y (2009): Static and dynamic characteristics of cerebral blood flow during the resting state. Neuroimage 48:515–524.

Zou QH, Zhu CZ, Yang Y, Zuo XN, Long XY, Cao QJ, Wang YF, Zang YF (2008): An improved approach to detection of amplitude of low-frequency fluctuation (ALFF) for resting-state fMRI: Fractional ALFF. J Neurosci Methods 172:137–141.

Zuo XN, Di Martino A, Kelly C, Shehzad ZE, Gee DG, Klein DF, Castellanos FX, Biswal BB, Milham MP (2010): The oscillating brain: Complex and reliable. Neuroimage 49:1432–1445.